sustainability

MDPI

Article

Combination of Photo-Fenton and Granular Activated Carbon for the Removal of Microcontaminants from Municipal Wastewater via an Acidic Dye

Paula Núñez-Tafalla *, Irene Salmerón, Silvia Venditti and Joachim Hansen

Faculty of Science, Technology and Medicine, University of Luxembourg, 6 Rue Richard Coudenhove-Kalergi, 1359 Luxembourg, Luxembourg; irene.salmeron@uni.lu (I.S.); silvia.venditti@uni.lu (S.V.); joachim.hansen@uni.lu (J.H.)

* Correspondence: paula.nunez@uni.lu

Abstract: Combining photo-Fenton and granular activated carbon (GAC) is an alternative to increase the feasibility of using photo-Fenton in full scale. This work is a preliminary study of its viability at natural pH. Both technologies were applied separately and compared with their combination, GAC filtration instead of batch mode, to achieve an approach close to full scale. The target compound considered in this investigation was indigo carmine as a hydroxyl radicals' probe. The results show that 80% removal of the target compound could be achieved when 20 min of the photo-Fenton treatment time was applied with the optimal dosing of the reagents (5 mg L^{-1} of iron and 40 mg L^{-1} of $H2O_2$) working at natural conditions and using ethylenediamine-N,N-disuccinic acid as a chelating agent. Two GAC types, fresh GAC and regenerated, were evaluated on Rapid Small-Scale Columns showing similar breakthroughs and close capacity to adsorb the target compound per gram of GAC. Combining the technologies, with photo-Fenton as the first step and GAC as the second, was performed with 5 min of photo-Fenton treatment time. The 80% removal was maintained during 340 and 170 bed volumes for fresh and regenerated GAC, respectively. Aiming to achieve the maximum reduction of irradiation, 75% of the energy consumption was saved compared to the standalone photo-Fenton process, and the GAC life was extended to a maximum of 7 times.

Keywords: advance oxidation processes; micropollutants; process combination; tertiary treatment; water remediation

Citation: Núñez-Tafalla, P.; Salmerón, I.; Venditti, S.; Hansen, J. Combination of Photo-Fenton and Granular Activated Carbon for the Removal of Microcontaminants from Municipal Wastewater via an Acidic Dye. *Sustainability* **2024**, *16*, 1605. https://doi.org/10.3390/su16041605

Academic Editor: Vito Rizzi

Received: 15 January 2024
Revised: 5 February 2024
Accepted: 6 February 2024
Published: 14 February 2024

1. Introduction

In recent years, the presence of contaminants of emerging concern (CECs) from municipal wastewater effluents in the receiving water bodies has increased [1]. These anthropogenic organic substances are present at trace levels; however, they can represent a severe risk to the environment and human health [2]. As conventional wastewater treatment plants (WWTPs) are not designed to degrade them [3,4], upgrading them with further steps is necessary to avoid widespread CECs.

In response to this concern, the European Commission (EC) established a watchlist of those CECs that are suspected to pose a hazard to the environment (Directives 2000/60/EC, 2008/105/EC and 2013/39/EU). This regulation is updated periodically, setting progressively more restrictive limits for their discharge. Like in other EU Member States, the Water Management Authority of Luxembourg (Administration de la Gestion de l'Eau) is adopting in its own regulation based on those European Directives, applying more severe regulations regarding the mitigation of CEC emissions with the attempt to achieve a better status of surface water bodies. The Luxemburgish guidelines to implement a post-treatment step were released in June 2020. They state the need to achieve 80% elimination of four selected CECs between the inlet of the WWTP and the outlet.

Advanced Oxidation Processes (AOPs) are powerful technologies for the purification of secondary treatment effluents, which are based on the generation of hydroxyl radicals ($^{\bullet}OH$). They have a very short lifetime (10^{-9} s [5]) but are highly reactive in a non-selective way with organic molecules; thus, they can degrade recalcitrant and persistent compounds and even mineralise them.

Among all the AOPs, photo-Fenton has shown promising results due to its efficiency in removing CECs [6]. It is based on an upgrade of the Fenton reaction (Equation (1)), using photons to regenerate the Fe^{3+} to Fe^{2+}, simultaneously producing a higher amount of $^{\bullet}OH$ (Equation (2)).

$$Fe^{2+} + H_2O_2 \rightarrow Fe^{3+} + OH^- + {}^{\bullet}OH \quad (1)$$

$$Fe^{3+} + H_2O + hv \rightarrow Fe^{2+} + {}^{\bullet}OH + H^+ \quad (2)$$

The main drawback of this technology is the low pH required to keep iron in the solution (optimal pH 2.8) and avoid slurry generation. As a consequence, the research focused on working at a neutral pH. The main advantages are avoiding the costs of acidification and later neutralisation and the increase in the effluent's salinity [7]. As a downside, a neutral pH requires chelating agents [8] to maintain the iron dissolved. Ethylenediamine-N,N-disuccinic acid (EDDS) offers a suitable solution in terms of chelate stability and treatment time, it allows achieving more than 80% removal in a short treatment time at low iron doses [9]. Its optimal pH range is between 3 and 7, but even in a weak basic medium, it is possible to reach high removal rates, e.g., almost 80% of cyclophosphamide and up to 90% of 5-fluorouracil [10], both cytostatics with high ecotoxicological potential.

Recently, nitrilotriacetic acid (NTA) has also been proposed as a chelating agent. Via using NTA, the removal rate for carbamazepine, ibuprofen, or crotamiton reaches more than 92% when illuminated with a UVA lamp [11]. The removal rate when using NTA compared with the use of EDDS at a continuous flow and medium scale (around 100 L) is demonstrated to be lower, despite the fact that at a small scale (until 20 L), similar behaviour is reported. This drawback is, however, compensated by the NTA's remarkably lower price.

Despite the successful results with photo-Fenton, it still has high costs in terms of reagents and energy consumption. In this context, combining the photo-Fenton process with other technologies is currently considered [12]. This work proposes the combination of photo-Fenton with activated carbon filtration to reduce the dosage of reagents and the hydraulic retention time (HRT).

Technologies based on separation are also very effective for water treatment. Granular activated carbon (GAC) filtration has been deeply investigated since it does not generate toxic by-products and is easy to implement, operate and maintain [13]. The adsorption of CECs depends on the dissolved organic matter, the physical–chemical properties of each CEC, the contact time and the physical–chemical properties of the influent [14,15]. Nonetheless, the use of GAC revealed two main disadvantages: the high cost of its replacement and the environmental impact produced in terms of carbon footprint [16].

To minimise both GAC drawbacks, regenerated GAC is considered as a replacement when the fresh material is depleted [17]. Different regeneration methods have been investigated but, in all cases, the initial GAC's properties changed, reducing its efficiency. Larasati et al. (2022) [18] reported that a 21% reduction in efficiency was obtained in the first regeneration cycle and 64% in the fourth cycle. However, this efficiency reduction is compensated by the cost and environmental impact reductions [19].

Commonly, adsorption experiments testing GAC require a long operation time for their correct evaluation, since a fixed bed column usually contains a large amount of material with a high adsorption capacity, even at the laboratory scale. Some CECs, such as metaldehyde and isoproturon, achieve the breakthrough after between 50,000 and 100,000 bed volumes (BV) with fresh GAC [18]. Aiming at reducing experiment duration but still providing reliable data, Crittenden et al. (1986) [19] designed a "Rapid Small-Scale Column (RSSC)" concept, minimising the volume of GAC and water used in every experiment,

which allows the process to reach the breakthrough within days of operation rather than months. The obtained results can be transferred to scale up accurately and reliably.

The combination of photo-Fenton and GAC could be an attractive option for CEC depuration since it would allow reducing the treatment time and reagent dosage of the photo-Fenton process, and it could extend the lifetime of the subsequent GAC step while still providing a high removal rate.

The combination of the two processes has been rarely studied. In the few studies available, photo-Fenton was operated at an acidic pH and at a laboratory scale [20,21], far away from the conditions and needs of a WWTP. Further, in those studies [20,21], GAC adsorption was studied in batch mode in contrast to the filtration performed in this work, which is the usual operation in bigger scales. The results showed the removal of up to 95% [20] and 90% [21] for antibiotics and cytostatics (i.e., Flutamide), respectively. Therefore, the combined treatment could be a suitable alternative when tested under realistic conditions: operating at a natural pH and real matrix, using both fresh and regenerated GAC sources as the scope of this work. The objective is to implement it as a post-treatment step in the WWTP of Heiderscheidergrund (12,000 population equivalent, Esch-sur-Sûre, North of Luxembourg).

Considering the complexity of the individual technology, the combination of both processes was calibrated with indigo carmine as a model compound for organic pollutants [22,23], known to be a suitable dye and an $^{\bullet}$OH probe in photocatalysis [24]. Its use to compare the adsorption capacity of different GAC types has been widely reported [25]. Indigo carmine is one of the most used dyes, from the textile industry to the food industry; up to 40 thousand tons of indigo carmine are produced annually [26]. It is a toxic dye that can affect human health; it can cause various pathologies such as hypertension, respiratory tract diseases and skin irritations [27]. The management of wastewater containing indigo carmine poses a challenge due to the intricate aromatic molecular structures.

Thus, this work aimed to study the viability of the removal of textile dyes from a treatment plant using the combination of photo-Fenton and GAC filtration processes. The specific objectives of this study were: (i) to determine the best working conditions of photo-Fenton and GAC technologies and (ii) to compare the efficiency of the technologies separately and combined. Several reagents' concentrations, chelating agents, and types of lamps were studied for the photo-Fenton. Fresh and regenerated GAC were compared in terms of efficiency in indigo carmine removal. Last, the effect of the presence of photo-Fenton residual reagents on the efficiency of activated carbon filtration was also evaluated.

2. Materials and Methods

2.1. Chemicals

Indigo carmine (80% purity) from Carl Roth GmbH (Karlsruhe, Germany) was used as model compound. Ferric sulfate heptahydrate (97%), ammonium acetate (98%), orthophenanthroline (99%), ascorbic acid (99%), EDDS 35%), NTA (≥99%), titanium(IV)oxysulfate (15%), sodium thiosulfate (98%) and liver bovine catalase were acquired from Sigma-Aldrich (Steinheim, Germany). Hydrogen peroxide (35%), sodium hydroxide (99%), sulfuric acid (96%) and glacial acetic acid were supplied by Carl Roth GmbH (Karlsruhe, Germany).

2.2. Analytical Determinations

Indigo carmine concentration was measured with a DR3900 spectrophotometer from Hach-Lange at 608 nm. Iron concentration was determined by the spectrometric method using 1,10-phenanthroline (ISO 6332 method) at 510 nm, while hydrogen peroxide was quantified by a colorimetric method using titanium(IV)oxysulphate (DIN 38 402 H15) at 410 nm. pH was monitored with pHmeter pH 7 Vio from DOSTMANN electronics GmbH (Wertheim-Reich olzheim).

2.3. Matrix Characterisation

The experiments tested the removal of a solution of 25 mg L^{-1} of indigo carmine in two water matrices. The concentration was selected based on the literature, i.e., concentrations between 7 and 60 mg for AOP [28,29] and 30 and 60 mg L^{-1} for adsorption processes [30,31]. In the first investigation phase, the target compound was dissolved in deionised water. In the second phase, the matrix water was the effluent from the Heiderscheidergrund WWTP (Esch-sur-Sûre, Luxembourg) collected after the second clarifier. The main characteristics of the real wastewater were pH 7–7.2, 500–550 µS cm^{-1} of conductivity, 41–42 mg $CaCO_3$ L^{-1}, 9–14 mg L^{-1} of Chemical Oxygen Demand (COD), 10 mg L^{-1} of Total Nitrogen (TN), <0.02 mg L^{-1} of NH_4^+-N, 8 mg L^{-1} of NO_3^--N and 0.82 mg L^{-1} of total phosphorus.

2.4. Experimental Setup

2.4.1. Photo-Fenton System

The photo-Fenton system (Figure 1a,b) was designed and developed in collaboration with Enviolet GmbH (Germany). It consists of three borosilicate reactors connected in serial, each containing a different UV lamp. The lamps installed are two medium-pressure (MP) lamps of 500 W (marked with D in 1a) and 150 W (marked with C in Figure 1a, C) and a low-pressure (LP) lamp of 40 W (marked with B in Figure 1a, B). Irradiation profiles are provided in the Supplementary Information (SI) (Table S1). Each reactor has an irradiated volume of 1.2 L and an external surface of 0.1 m^2. The reactors are fed from a polyethylene tank (75 L capacity) connected to a Schmitt MPN115 (0.25 kW) centrifugal pump at a flow rate of 800 L min^{-1}, ensuring a turbulent regime inside the reactors. The temperature was maintained between 18 and 23 °C through two cooling coils to avoid lamps overheating.

The system was operated in batch mode, treating 60 L of solution each time. For the experiments, different lamps were used in single lamp configuration; besides that, the simultaneous use of MP and LP lamps was tested. The reactor was filled with the water matrix, adding 25 mg L^{-1} of indigo carmine, and recirculated for 15 min until homogeneity was reached. Afterwards, the iron complex was added, and the pH was then adjusted to simulate the natural pH of the wastewater. The time zero of the experiment was taken when the hydrogen peroxide was added and the lamps were switched on.

The iron complex was prepared by dissolving iron in acidic water until complete dissolution. Then, the chelating agent was added (molar concentration 1:1) to the iron solution and stirred until the complete complex formation, being EDDS or NTA.

The treatment time was established to be 20 min in batch mode, resulting in 0.4 min of "relative contact time" (meaning the time that the effluent has been inside the lamp, or rather the irradiation time) inside the borosilicate reactor. This setup intended to simulate the real operational time ranges of HRT in a continuous process at full scale, which usually isin the order of seconds [32,33]. The residual H_2O_2 of each sample was quenched with a solution of 1 g L^{-1} of bovine catalase to stop the Fenton reaction.

2.4.2. Granular Activated Carbon Behaviour (Adsorption Determination)

The first phase of the GAC tests was designed to characterise their (regenerated and fresh GAC) behaviour. Concentrations between 0.1 and 1 g L^{-1} of both GACs were in contact with a 25 mg L^{-1} indigo carmine solution in 250 mL amber glass bottles in constant stir. The GAC was not previously washed and no other pre-treatment was performed, to simulate its use on a real scale.

The influence of the residual reagents of photo-Fenton was studied in a solution of 25 mg L^{-1} of indigo carmine with 1 g L^{-1} GAC. Ten tests were carried out with hydrogen peroxide between 0 and 50 mg L^{-1} and iron between 0 and 5.5 mg L^{-1} (Table S2). Indigo carmine, iron and H_2O_2 concentrations were measured for 24 h.

The two GACs tested were CarboTech DGF 8x30 GL (Carbo Tech AC GmbH (Essen, Germany)) as fresh source and reference material and NRS Carbon GA 0.5–2.5 GAC (Cabot Norit Netherlands BV) as regenerated one (Figure S1). The main physicochemical properties of both are shown in Table S3.

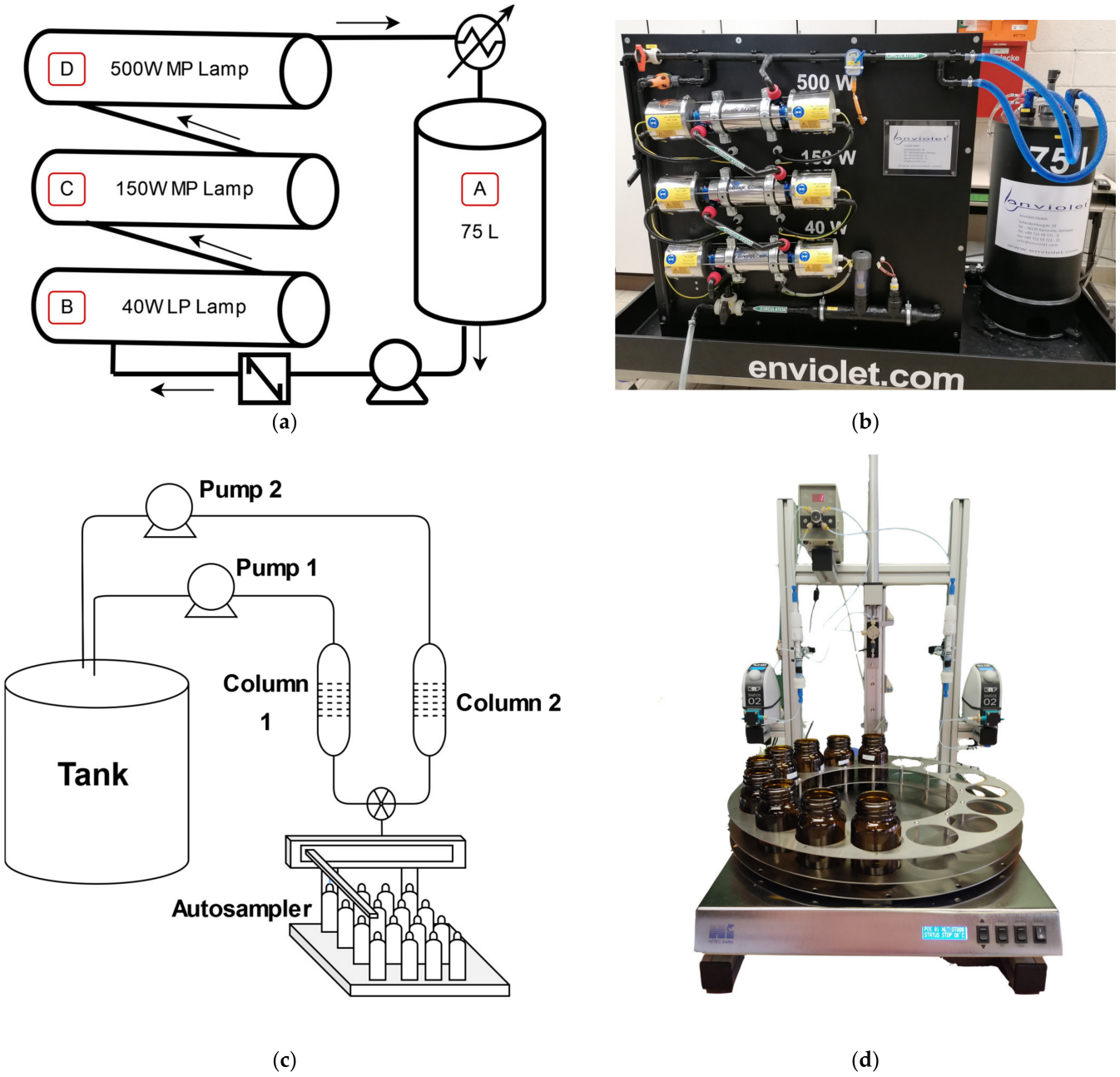

Figure 1. Equipment schemes and pictures. Photo-Fenton equipment (**a**) scheme, (**b**) picture. RSSC equipment, (**c**) scheme, (**d**) picture. Symbols of (**a**,**b**) arrows show the flux. A: tank, B: 40 W LP Lamp, C: 150 W MP Lamp, D: 500 W MP lamp.

2.4.3. Granular Activated Carbon Rapid Small-Scale Columns Test

The second phase addressed the indigo carmine removal capacity by GAC using RSSC to obtain the breakthrough in a short period of time. The design of the RSSC (Figure 1c,d) was based on the study of Zietzschmann et al. [34]. It consisted of two glass columns with a BV in 1 mL of GAC. The columns were fed with a diaphragm pump (KNF Simdos 02, KNF DAC GmbH (Hamburg, Germany)) with a 10 mL min^{-1} flow, meaning a contact time of 6 s. The treated water samples were taken at defined times by an autosampler (AutoSam 2.3, HiTec Zang GmbH (Herzogenrath, Germany)). GAC was crushed and sieved to obtain uniform size between 100 and 500 µm. Crushed GAC was rinsed with deionised water and dried; then, it was placed in the columns using glass wool at the ends to hold GAC in place.

A 50 L tank fed the system with the water matrix, deionised or real effluent, in each case containing 25 mg L^{-1} of indigo carmine.

2.4.4. Combination of Photo-Fenton Process and Granular Activated Carbon

The combination of treatments was performed with real wastewater. The polluted solution was treated by photo-Fenton and, straight after, by GAC in RSSC. The photo-Fenton test was performed under the best conditions obtained previously. The treatment time was selected based on the removal ratios reached in the previous test. Lamps were switched off after the reaction time, and sodium thiosulfate was added in excess to stop the reaction. Then, the water was transferred to the columns' feeding tank, and the same procedure as previously was carried out.

2.5. Methods

2.5.1. Optimization by Response Surface Methodology

Response Surface Methodology (RSM) was applied to investigate the influence of the variation of the inputs of the system, mainly reagent dosages, in the contaminants removal response, aiming to establish the optimal operational conditions. A two-factor central composite design was carried out, with an alpha of 1.19 (Table S4).

The design of experiments proposed 10 runs, in which different iron and peroxide concentrations were tested and selected according to common values reported in the literature [35]. The iron and H_2O_2 concentrations were established by RSM, being the low and high iron concentrations in 3 and 10 mg L^{-1}, respectively, and H_2O_2 in 10 and 50 mg L^{-1}. Detailed RSM factor values are indicated in Table S4. Table S5 includes the experimental design and the indigo carmine removal.

The experimental design was performed with two different lamps, 500 W MP and 40 W LP, to compare the possible differences in the system's behaviour according to the two irradiation profiles.

2.5.2. Curve Fitting of the Adsorption Breakthrough

The breakthrough obtained with the RSSCs for every GAC profile as function of the BV was modelled via curve fitting. The breakthrough was defined following Wroch [36] definition, as the time between C/C_0 equals to 0.05 and 0.95. The BV is a dimensionless parameter defined as in Equation (3) [36]. The modelling was performed according to two different approaches: under the hypothesis that the adsorption of the model compound follows a first-order kinetic [37] and under the hypothesis of a second-order kinetic [38]. The best-fitting model will allow a proper comparison between the materials.

$$BV = \frac{V_{Feed}}{V_R} = \frac{t}{EBCT} \quad (3)$$

where V_{Feed} is the volume fed (mL), V_R is the adsorbed volume (mL), t is time (min) and EBCT is the empty bed contact time (min).

The fitting with a first-order kinetic was carried out by the model described in Equation (4):

$$G = \frac{q\,K\,BV}{1 + K\,BV} \quad (4)$$

where G is the amount of the model compound per gram of GAC, q and K are adsorption parameters and BV is the BV at which the effluent concentration is measured.

For the second-order kinetics, the proposed model is stated in Equation (5):

$$\frac{C}{C_0} = \frac{1}{1 + e^{(A - B\,t)}} \quad (5)$$

where C is the concentration at time t, C_0 is the initial concentration, A and B are adsorption parameters and t is time.

The viability of the model is evaluated by the regression coefficient (square of the Pearson Product-Moment Correlation Coefficient) R^2. Values closer to 1 mean more representative data.

3. Results and Discussion

3.1. Photo-Fenton

3.1.1. Determination of the Optimised Operational Conditions

The results of the RSM are summarised in Table S5. In all the tested scenarios, the 500 W MP lamp reached a high indigo carmine removal, in some cases more than 95%, achieving even 97.5% when dosing 6.5 mg L^{-1} of iron and 54 mg L^{-1} of H_2O_2, while the 40 W LP lamp reached only 49.5% with the maximum iron and H_2O_2 dosage. The lower performance of the 40 W LP lamp may be caused by its lower power and nature. In fact, the 40 W LP lamp emits only in the UVC spectrum, and the regeneration of Fe^{+3} to Fe^{+2} occurs mainly between 314 and 360 nm (UVA). As such, a broad-spectrum lamp would be more effective [39].

The correlation between the two independent variables (iron and H_2O_2) and the response (indigo carmine removal) is modelled in Equations (6) and (7). The 500 W MP lamp followed a quadratic trend (6), and the 40 W LP lamp followed a linear trend (7). Consequently, the target compound removal on the 500 W MP lamp did not always increase as the reagent's dosage rose, whereas, with the 40 W LP lamp, the target compound removal increased as the reagent's dosage rose. Both models were carried out by an analysis of variance (ANOVA), and the summarised results are in Table 1. The F-value shows that both models are significant, and the likelihood that these results are due to noise is less than 0.5%.

Table 1. ANOVA values for RSM of 500 W MP and 40 W LP lamps.

Source	Sum of Square	Degree of Freedom	Mean Square	F-Value	*p*-Value	
500 W MP Lamp						
Quadratic model	1581.88	5	316.38	96.68	0.003	Significant
A-Iron	870.92	1	870.92	266.14	<0.0001	
B-H_2O_2	333.48	1	333.48	101.91	0.0005	
AB	5.64	1	5.64	1.72	0.2595	
A2	330.88	1	330.88	101.11	0.0006	
B2	97.71	197.71	29.86	0.0055		
Residual	13.09	4	3.27			Not significant
Lack of fit	8.94	3	2.98			
Pure error	4.15	1	4.15			
40 W LP Lamp						
Lineal model	944.07	2	472.04	12.54	0.0048	Significant
A-Iron	681.81	1	681.81	18.11	0.0038	
B-H_2O_2	262.26	1	262.26	6.96	0.0335	
Residual	2.63.59	7	37.66			
Lack of fit	261.55	6	43.59	21.37	0.1641	Not significant
Pure error	2.04	1	2.04			

The fitting of the quadratic model (500 W MP lamp) was adequate, with a regression coefficient (R^2) of 0.982. Nonetheless, the fitting of the 40 W LP lamp with the model was lower, with a R^2 of 0.72.

$$Y = 14.0 + 14.5*Fe + 1.3\times H_2O_2 - 0.02\ Fe\times H_2O_2 - 0.83\times Fe^2 - 0.01\times {H_2O_2}^2 \quad (6)$$

$$Y = 5.66 + 12.85\times Fe + 0.31\times H_2O_2 \quad (7)$$

The 3D response surface plots (Figure 2) allow a better analysis of the behaviour of the treatment when the variables change, making it easy to identify the influence of each variable on the indigo carmine removal.

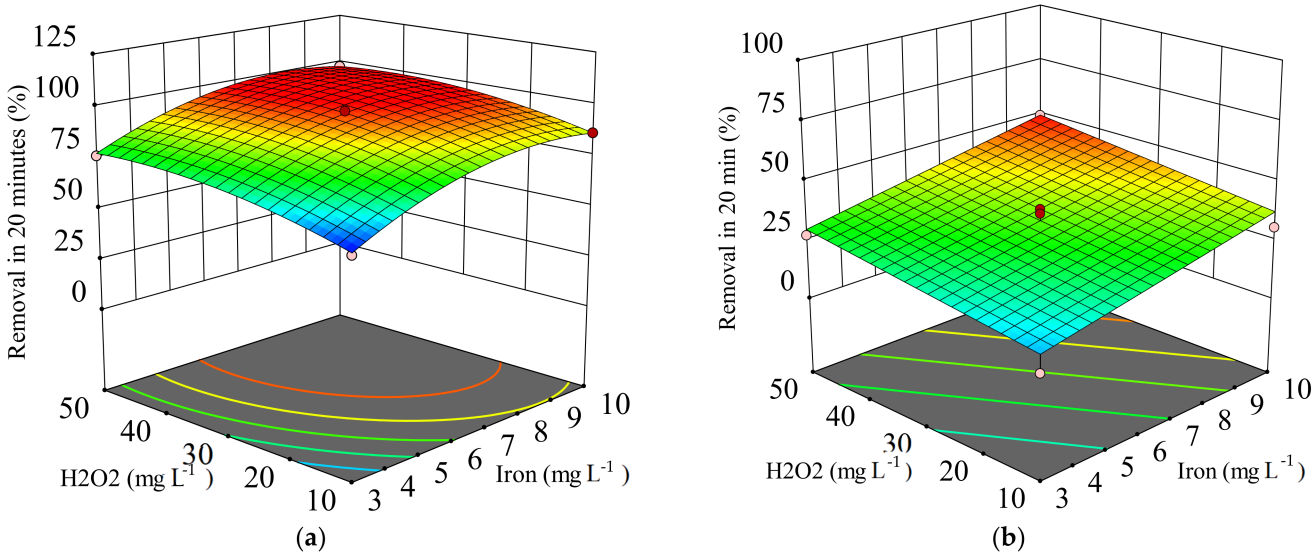

Figure 2. Response–surface plot and experimental values (circles) show the influence of iron and H_2O_2 dose to remove the pollutant. (**a**) 500 W MP Lamp, (**b**) 40 W LP lamp.

Results of the 500 W MP lamp (Figure 2a) showed that a slight variation in iron can significantly affect the removal of the model compound. 3 mg L^{-1} of iron and 10 mg L^{-1} of H_2O_2 reached 60% while increasing the iron to 4 mg L^{-1}, keeping the same quantity of H_2O_2, reached 70%. However, the elimination attained its maximum ratio at a concentration of 7 mg L^{-1} of iron. Above this value, the removal of indigo carmine reained constant or even decreased. That can be attributed to a scavenging effect of the $^{\bullet}OH$ caused by a high photoreduction of Fe^{3+} [40].

A larger increase of H_2O_2 dosing was found necessary to generate a notable increase in the model compound removal. These results are in concordance with those obtained by other authors [41]. The removal of alprazolam increased as iron increased, until a concentration of 7.7 mg L^{-1}, and the same trend was observed with the H_2O_2 concentration until a concentration of 47.5 mg L^{-1} [35,41]. From the results, 50 mg L^{-1} of H_2O_2 appears to be the maximum value at which a positive effect can still be appreciated under the tested conditions with 500 W MP lamps.

Regarding the performance of the 40 W LP lamp (Figure 2b), it was observed that the removal rates increased when a higher H_2O_2 concentration was applied. The same trend was observed with the iron concentration. The ANOVA model confirmed that the 40 W LP lamp follows a linear model. The optimised dose with the aim of increasing the target compound removal and decreasing the reagent's dosage was 6.5 mg L^{-1} of iron and 30 mg L^{-1} for the 40 W LP lamp.

Once the behaviour of each lamp was known, the optimal conditions were defined as the ones achieving the highest pollutant elimination (minimum 80%) while using as little iron and H_2O_2 dosage as possible.

According to that premise, the most favourable irradiation was achieved with the 500 W MP combined with an optimal dosage of iron and H_2O_2, 6.3 and 24 mg L^{-1}, respectively. These results were promising since a reduction of reactants was achieved regarding previous works [42]. Cuervo Lumbaque et al. [43] obtained similar behaviour despite their optimal concentrations being significantly higher (iron was 15 mg L^{-1} and H_2O_2 90 mg L^{-1}) than the ones obtained in this study. They also worked at circumneutral pH.

The obtained optimal iron dose and its subsequent discharge can be considered too high for a real application of the technology, since few German regions recommend

maintaining between 0.7 and 1.8 mg L^{-1} [44] the iron concentration in the receiving water bodies. Previous works reported a satisfactory •OH yield for the removal of CECs with 5.5 mg L^{-1} of iron [45]. For that reason, the iron was limited to 5.5 mg L^{-1}, obtaining an optimal adapted dosage of 5 mg L^{-1} of iron and 40 mg L^{-1} of H_2O_2.

An additional experiment was carried out to validate the optimisation. The removal obtained was close to the model extrapolation, with a difference lower than 5%. In this assay, both COD and TN were monitored, resulting in the COD content slightly decrease and TN remaining constant.

3.1.2. Simultaneous Application of MP and LP Lamps

Expecting to improve the previous scenarios, the simultaneous use of both lamps was tested, searching for synergies between the two systems. The addition of the 40 W LP lamp was added as a preprocessing stage to increase the treatment efficiency, aiming at better usage of the reagents.

The simultaneous use of both lamps (500 W MP + 40 W LP lamp) was carried out under the optimal conditions for the 500 W MP lamp: 5 mg L^{-1} of iron and 40 mg L^{-1} of H_2O_2. The time to achieve the target, 80% removal, was reduced to 15 min, meaning 0.3 min of relative contact time (Figure 4a). As the required treatment time was diminished, a reduction in the dosage of reagents, mainly iron, was also tested to minimise their discharge into the environment. With 3 mg L^{-1} of iron maintaining the 40 mg L^{-1} of H_2O_2, the time to reach 80% removal increased to 20 min, while, for 5 mg L^{-1} of iron, 80% removal was achieved in 15 min. The difference in irradiation time between both scenarios was 0.1 min—this increase is acceptable for the scale-up. Therefore, to find a compromise between iron dosage and treatment time, 3 mg L^{-1} of iron, maintaining the 40 mg L^{-1} of H_2O_2, was selected as the most suitable.

3.1.3. Comparison of the Photo-Fenton Process: LP lamp, MP Lamp and Simultaneous Application of MP and LP Lamps

The removal of the model compound by photo-Fenton was compared across the three different lamp alternatives (Figure 4b) to select the most suitable scenario. The optimised working condition for each lamp was selected from the previous test as follows: 5 mg L^{-1} of iron and 40 mg L^{-1} for the 500 W MP lamp; 6.5 mg L^{-1} of iron and 30 mg L^{-1} for the 40 W LP lamp; and 3 mg L^{-1} of iron and 50 mg L^{-1} for the combination of both lamps.

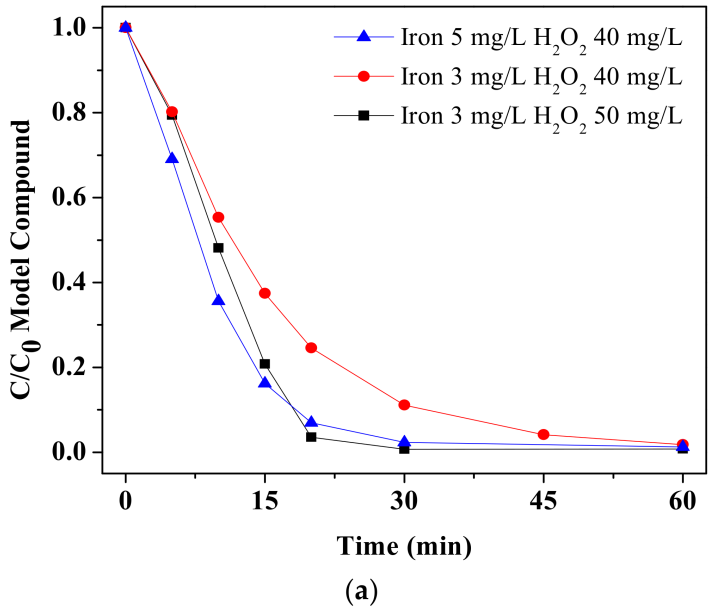

Figure 3. *Cont.*

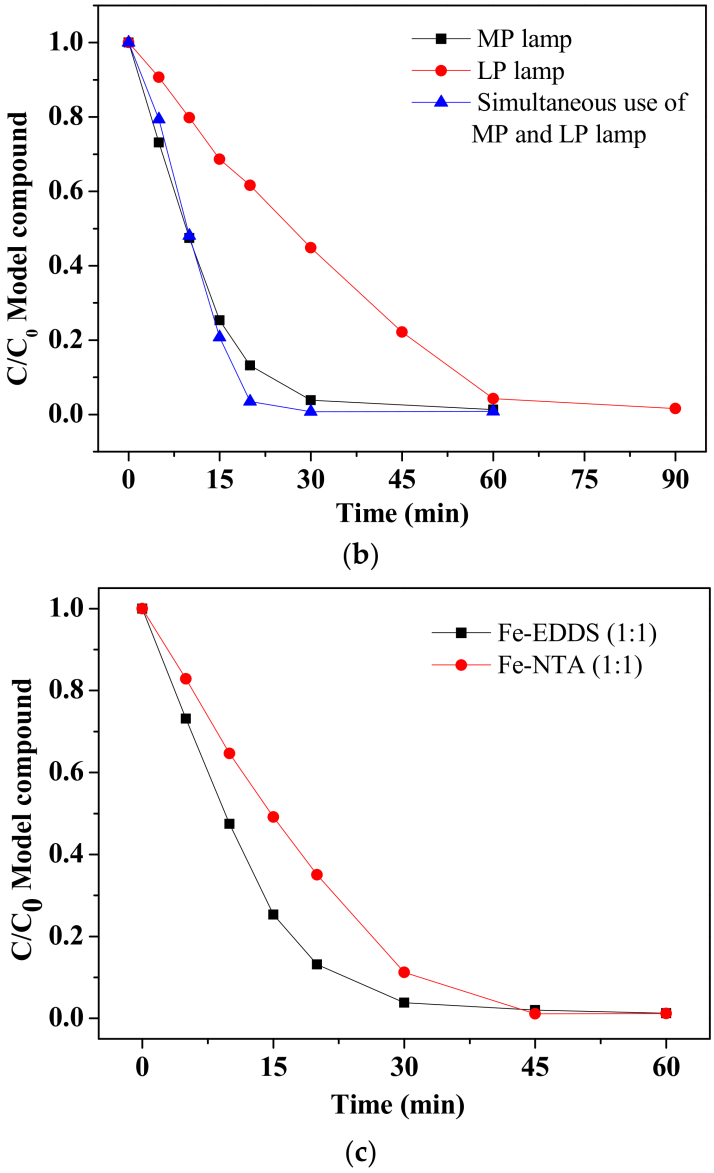

Figure 4. Indigo carmine removal trend during photo-Fenton process. [indigo carmine]$_0$ = 25 mg L^{-1}, pH$_0$ = 7.1–7.2, t$_0$ = 19–20 °C. (**a**) Combination LP and MP lamps for the different initial H_2O_2 and iron concentrations. (**b**) Comparison of different lamp possibilities: 500 W MP lamp, iron = 5 mg L^{-1}, H_2O_2 = 40 mg L^{-1}; LP lamp, iron = 6.5 mg L^{-1}, H_2O_2 = 30 mg L^{-1}; simultaneous use of lamps, iron = 3 mg L^{-1}, H_2O_2 = 50 mg L^{-1} (**c**) Comparison of two different chelating agents: 500 W MP lamp, iron = 5 mg L^{-1}, H_2O_2 = 40 mg L$^{-1.}$.

Figure 4b shows that the simultaneous application of the lamps and the 500 W MP lamp as a stand-alone had similar yields despite the treatment with both lamps being slightly quicker. On the contrary, the 40 W LP lamp alone shows remarkably slower removal rates; due to its lower power, it has a lower energy consumption.

Nevertheless, the 40 W LP lamp was the best option if the removal vs. energy consumption (on nominal values) was considered, as the lower power of the LP lamp has a lower energy consumption. More than 5 times the energy consumption was needed to achieve the 80% removal of the reference compound by the 500 W MP lamp or the combination (30 Wh on the 40 W LP lamp and 167 Wh on the 500 W MP lamp) compared to the 40 W LP lamp. The slight increase of the target compound removal of the combination of lamps, with respect to the 500 W MP lamp stand-alone, did not justified the use of the combination of lamps due to the increment of energy consumption.

Thus, considering that long HRT is required for the 40 W LP lamp, the 500 W MP lamp was selected.

3.1.4. Chelating Agents' Assessment

Finding the best chelating agent is currently one of the focuses of the scientific community researching the photo-Fenton process at circumneutral pH. Recently, the interest in using NTA to keep iron in the solution has grown since it can form strong ligands with Fe^{3+}, remaining dissolved at pH 7 and has a lower cost than EDDS [11,46]: the NTA (analytical compound) cost is 90% less than EDDS. Thus, the comparison between EDDS and NTA was also addressed.

The 500 W MP lamp with the optimal reagents' dosages was selected to study them. The results showed a considerable difference in removal rates between EDDS and NTA. Using EDDS, the 80% removal of indigo carmine was achieved in 20 min, while, with NTA, 30 min were needed (Figure 4c). It means an increase in relative contact time from 0.4 minutes when EDDS was used to 0.6 minutes with NTA. Iron dissolved in both experiments remained constant until the target removal was achieved. It can be explained by the higher photoactivity of EDDS, which makes its decomposition faster, generating a higher amount of Fe^{2+} available to react and generate $^{\bullet}OH$ [47].

3.2. Granular Activated Carbon

3.2.1. GAC Behaviour (Adsorption Determination)

With the lowest concentration of both GACs, 0.1 g L^{-1}, 15% of the indigo carmine was adsorbed after 24 h. The capacity to adsorb the model compound increased as the GAC concentration increased. In 9 h, adding 1 g L^{-1} of GAC, more than 65% of the indigo carmine was removed when CarboTech DGF 8x30 GL was used, and almost 60% was achieved using NRS Carbon 0.5–2.5. Up to 80% was achieved with both GACs in less than 24 h, being attained approximately after 13 h.

The behaviours of the two GACs were similar (Figure 5), and the trend for each concentration was analogous. A slight difference between the two materials was observed in favour of fresh GAC; several authors have reported a similar efficiency in fresh and regenerated GAC in the literature [48].

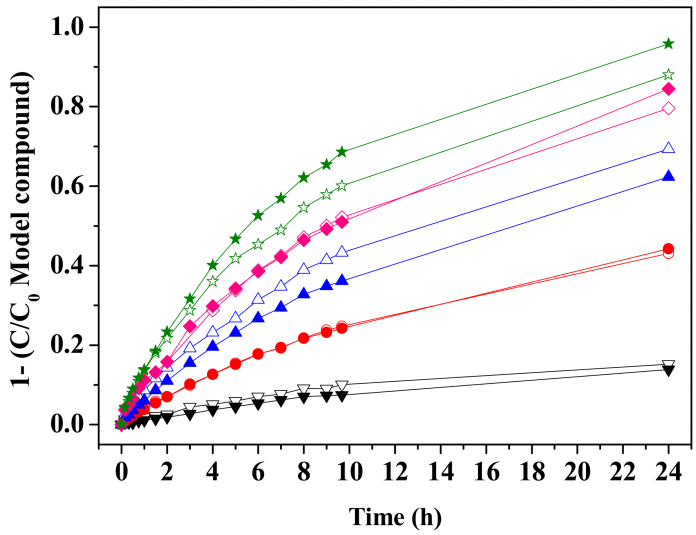

Figure 5. Adsorption of indigo carmine by GAC. Solid symbols: CarboTech DGF 8x30 GL. Open symbols: NRS Carbon 0.5–2.5. ▼ 0.1 g L^{-1} GAC, ● 0.3 g L^{-1} GAC, ▲0.5 g L^{-1} GAC, ◆ 0.75 g L^{-1} GAC, ★ 1 g L^{-1} GAC.

3.2.2. Rapid Small-Scale Columns

The RSSC test is a confirmed method used to predict the breakthrough on full-scale GAC columns [49]. The adsorption profile curve was performed for CarboTech DGF 8x30 GL and NRS Carbon 0.5–2.5 (Figure 6). The implementation of the kinetic models was necessary to compare both GACs properly.

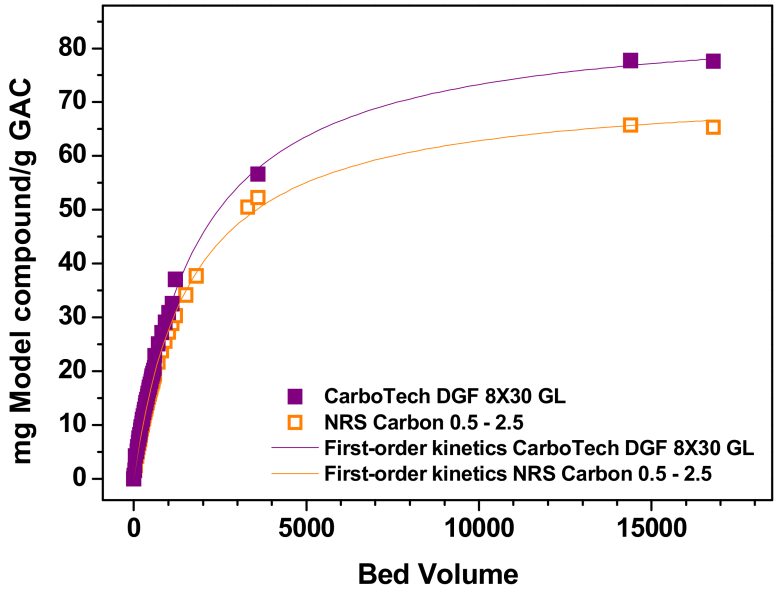

Figure 6. Modelled adsorption of indigo carmine in the RSSC under the first-order kinetics hypothesis.

The curve fitting for the first- and second-order kinetics is presented in Figure S2 for both GAC types. The coefficient of determination (R^2) was also calculated to select the best-fitting model. In the case of the first-order kinetic model, the R^2 was 0.992 and 0.999 for CarboTech DGF 8x30 GL and NRS Carbon 0.5–2.5, respectively. Contrary, the R^2 of the second-order kinetics were 0.884 and 0.897 for CarboTech DGF 8x30 GL and NRS Carbon 0.5–2.5, respectively (Table 2). The significantly higher R^2 of the first-order kinetics models evidenced their high accuracy for describing the adsorption process. Thus, the first-order kinetics model was selected to compare the two GAC types, and the second-order kinetics hypothesis was discarded. The constant values of the first-order kinetics model are shown in Table 2. They can be used as adsorption parameters to describe the adsorption process when different materials are compared. The calculated q shows the maximum amount of model compound adsorbed per mass of GAC; CarboTech DGF 8x30GL is the one with the higher capacity.

Table 2. Constant values of the first- and second-order kinetic models.

		CarboTech DGF 8x30 GL	NRS Carbon 0.5–2.5
First-order kinetic	q	86.38	73.21
	K	5.601×10^{-4}	6.069×10^{-4}
	R^2	0.992	0.999
Second-order kinetic	A	0.477	0.479
	B	0.016	0.018
	R^2	0.884	0.897

Our results are in line with previous ones, which reported that CarboTech DGF 8x30GL was able to adsorb approximately 80 mg of model compound per gram of GAC, while NRS Carbon 0.2–2.5 adsorbs around 65 mg g^{-1}. Better fresh GAC performance was expected, as regenerated GAC usually has a lower efficiency [50]. However, even with a 15% lower q, regenerated GAC can be considered a suitable alternative for its lower environmental impact.

3.3. Real Wastewater

3.3.1. Photo-Fenton

The scavengers present in the water, such as phosphate, carbonates or organic matter, reduce the removal efficiency of the photo-Fenton process. Han et al. [51] found that oxytetracycline elimination was inhibited up to 20% by the presence of 10 mM of phosphates or 10 mM of carbonates, and the tetracycline removal was around 10% lower in their presence. A similar trend was found by Cuervo Lumbaque et al. [52], who reported that diazepam, fluoxetine, paracetamol and progesterone removal decreased between 40 and 60%, although other compounds such as furosemide and dipyrone did not show a significant difference in elimination.

This phenomenon also happened in our investigations, where 5 mg L^{-1} of iron and 40 mg L^{-1} of H_2O_2 with 500 W MP lamps was tested. A total of 72% of the target compound was removed after 20 min of the photo-Fenton process was applied for real wastewater at optimum conditions (Figure S3). The 80% removal was achieved in less than 30 min of the process, meaning less than 36 s of irradiation. Iron remained dissolved in the solution during the whole experiment, while H_2O_2 was consumed by 10 mg L^{-1}.

3.3.2. Rapid Small-Scale Columns

As for the photo-Fenton process, the higher complexity of real wastewater hinders the GAC treatment performance since more species are competing for adsorption. The breakthrough curves for CarboTech DGF 8x30 GL and NRS Carbon 0.5–2.5 are plotted in Figure 7. The adsorption capacity was slightly reduced; therefore, the breakthrough was achieved slightly earlier than expected. For example, for NRS Carbon 0.5–2.5, a 50% breakthrough was achieved after 180 BV. In the case of the CarboTech DGF 8x30 GL, the 50% breakthrough was achieved after 280 BV. The 20% breakthrough, that means the maximum time in which the 80% removal is achieved, is 40 and 30 BV for CarboTech DGF 8x30 GL and NRS Carbon 0.5 – 2.5, respectively.

The first-order kinetic was also applied to model the adsorption. The model fitted for both GAC being the R^2 0.994 for both. With real wastewater, the CarboTech DGF 8x30 GL was able to adsorb approximately 70 mg g^{-1}; for the NRS Carbon 0.5–2.5, it was almost 60 mg g^{-1}. The effect of a more complex matrix was similar for both GAC types, which slightly reduced the adsorption capacity by 7 and 12%.

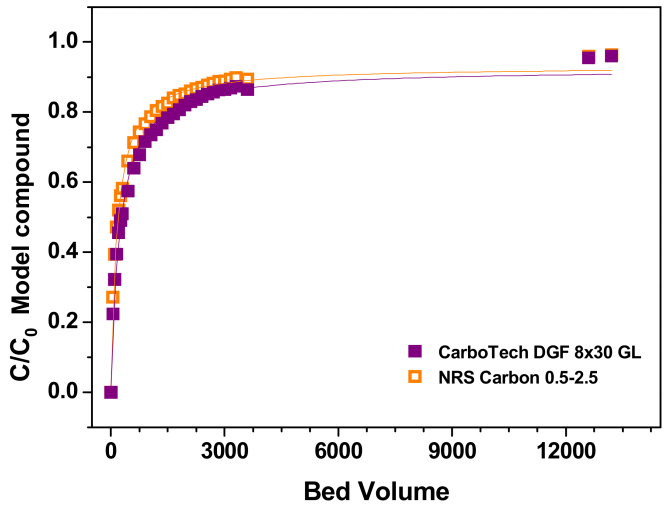

Figure 7. Modelled adsorption of indigo carmine in the RSSC under the first-order kinetics hypothesis in real wastewater,3.3.3. Photo-Fenton and GAC Combined Treatment on Real Wastewater.

The combination of technologies was implemented to reduce treatment time and reagent dosage in the photo-Fenton process and to extend the GAC's lifetime. The photo-Fenton process was applied as the first process for 5 min (6 s irradiation time). This

treatment time was selected to prioritise energy reduction, resulting in 75% energy savings. The conditions of the photo-Fenton were the optimal ones, 5 mg L^{-1} of iron chelated with EDDS in a molar ratio of 1:1 and 40 mg L^{-1} of H_2O_2 irradiated by a 500 W MP lamp.

The removal of indigo carmine achieved was 28%, resulting in a final concentration of 19 mg L^{-1}, and this solution fed the RSSC. The 50% breakthrough of CarboTech DGF 8x30 GL was reached after 1500 BV (Figure S4), and the 20% breakthrough was after 320 BV. For the NRS Carbon 0.5–2.5, the 50% breakthrough was 800 BV, and the 20% breakthrough was after 110 BV.

Compared with each process alone, photo-Fenton was reduced from 20 min to 5 min, meaning a nominal savings of 125 Wh in terms of irradiating energy. The GAC lifetime was extended almost 8 times for CarboTech DGF 8x30 GL and 6 times for NRS Carbon 0.5–2.5, defining a 50% breakthrough (Figure 8) as the breakthrough criterion. If the BV of 20% breakthrough is compared for both configurations, the GAC lifetime was extended almost 5 times and 7 times for CarboTech DGF 8x30 GL and NRS Carbon 0.5–2.5, respectively.

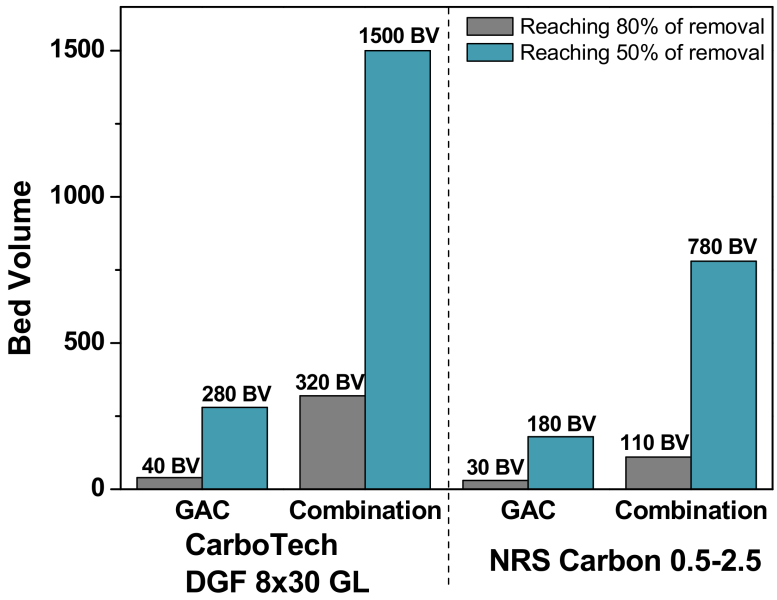

Figure 8. Bed volume achieved after reaching different target compound removal.

3.4. Economical Assessment

A preliminary cost assessment was performed to compare the economic feasibility of the three setups shown in this work. The compared conditions were the ones applied to real wastewater. The quality criterion required for comparing the processes was 80% removal of the model compound. On intensive processes, the most important parameter in terms of costs is operational expense (OPEX); on the contrary, for extensive processes, the most relevant cost is the capital (CAPEX). As both technologies are intensive processes, only the OPEX was considered.

The volume of treated water was 350 m^3 $year^{-1}$ based on Belalcázar-Saldarriaga et al. [53], who set it as a reference in a mid-scale textile industry environment. For photo-Fenton, the cost for electricity was 0.1 € kWh^{-1}; it was 0.325 € L^{-1} for the H_2O_2 solution 35%, 0.71 € L^{-1} for $Fe_2(SO_4)_3 \bullet H_2O$ and 3.5 € L^{-1} for EDDS (35% w/v) [54]. The GAC cost is estimated to be between 2100 and 2500 € ton^{-1} for fresh material and 1200 and 1600 € ton^{-1} for the regenerated material.

Table 3 shows the calculated price of each process per m^3. The most expensive was the photo-Fenton as a stand-alone technology. While the costs for the reagents were similar to those of the combination with GAC, the energy consumption was 6 times higher as a longer irradiation time was needed (33 s). The GAC filtration stand-alone was the cheapest, making the NRS Carbon GA 0.5–2.5 the most economically convenient. The GAC cost for the combination was slightly higher for the NRS Carbon GA 0.5–2.5 than the CarboTech

DGF 8x30 GL due to the quicker exhaustion of the first one. Facing the preliminary assessment, GAC columns seem the most suitable process with respect to the elimination of indigo carmine; however, a deeper study of other costs aside from operational ones (such as the disposal of the exhausted-not-regenerated GAC), environmental costs and risks should be carried out. The specific CECs will define the process capability for their removal (i.e., diclofenac was proven to be easily removed by photo-Fenton but not easily adsorbed in GAC), and so a quality criterion for limits of discharge could determine the final choice.

Table 3. Operational cost related to each tested scenario for the treatment of real wastewater.

	Photo-Fenton	**GAC Columns**		**Combination of Processes**	
		CarboTech DGF 8x30 GL	NRS Carbon GA 0.5–2.5	CarboTech DGF 8x30 GL	NRS Carbon GA 0.5–2.5
Energy (€/m^3)	0.059	--	--	0.010	0.010
GAC cost (€/m^3)	--	0.060	0.055	0.008	0.015
Reagents (€/m^3)	0.144	--	--	0.144	0.144
Total (€/m^3)	0.203	0.060	0.055	0.161	0.169

4. Conclusions

The results of this study suggest the suitability of combining the photo-Fenton process and GAC filtration to remove the textile dyes from a centralised treatment plant. This combination allows the reduction of the photo-Fenton treatment time and extends the GAC lifetime. The maximum reduction of irradiation energy consumption was 75%, and the GAC lifetime was extended by 5 to 7 times depending on the scenario, in both cases, compared to the use of the technologies independently. At the same time, the use of regenerated GAC to adsorb indigo carmine has been shown as a suitable alternative that will reduce the carbon footprint of the process. These results are promising and show that the combination of photo-Fenton and GAC filtration is an interesting alternative to make the scaling up of the photo-Fenton process feasible and more effective.

A natural progression of this work will be to evaluate this combination as a further step for the removal of representative CECs in Luxembourg. The two technologies independently and their combination will be studied at Heiderscheidergrund WWTP (Luxembourg) to assess their feasibility as an effective solution for urban effluent depuration.

Supplementary Materials: The following supporting information can be downloaded at https://www.mdpi.com/article/10.3390/su16041605/s1.

Author Contributions: P.N.-T.: Conceptualization, Investigation, Methodology, Visualization, Writing—Original draft preparation. I.S.: Conceptualization, Methodology, Validation, Writing—Review and Editing. S.V.: Conceptualization, Methodology, Writing—Review and Editing, Project Administration. J.H.: Writing—Review and Editing, Supervision, Project Administration, Funding Acquisition. All authors have read and agreed to the published version of the manuscript.

Funding: This research was funded by the Administration de la gestion de l'eau—Ministère du développement durable et des infrastructures of Luxembourg under the Fentastic Project.

Institutional Review Board Statement: Not applicable.

Informed Consent Statement: Not applicable.

Data Availability Statement: The datasets generated and/or analysed during the current study are available in the Supplementary Materials.

Acknowledgments: The authors wish to thank to our project partners SIDEN (Syndicat intercommunal de dépollution des eaux résiduaires du Nord), Hydro-Ingenieure, TR-Engineering and WiW (Wupperverbandsgesellschaft für integrale Wasserwirtschaft) mbh.

Conflicts of Interest: The authors declare no conflicts of interest.

References

1. Júnior, O.G.; Batista, L.L.; Ueira-Vieira, C.; Sousa, R.M.; Starling, M.C.V.; Trovó, A.G. Degradation mechanism of fipronil and its transformation products, matrix effects and toxicity during the solar/photo-Fenton process using ferric citrate complex. *J. Environ. Manag.* **2020**, *269*, 110756. [CrossRef] [PubMed]
2. Li, X.; Zhang, R.; Tian, T.; Shang, X.; Du, X.; He, Y.; Matsuura, N.; Luo, T.; Wang, Y.; Chen, J.; et al. Screening and ecological risk of 1200 organic micropollutants in Yangtze Estuary water. *Water Res.* **2021**, *201*, 117341. [CrossRef] [PubMed]
3. Grandclément, C.; Seyssiecq, I.; Piram, A.; Wong-Wah-Chung, P.; Vanot, G.; Tiliacos, N.; Roche, N.; Doumenq, P. From the conventional biological wastewater treatment to hybrid processes, the evaluation of organic micropollutant removal: A review. *Water Res.* **2017**, *111*, 297–317. [CrossRef] [PubMed]
4. Di Marcantonio, C.; Chiavola, A.; Dossi, S.; Cecchini, G.; Leoni, S.; Frugis, A.; Spizzirri, M.; Boni, M.R. Occurrence, seasonal variations and removal of Organic Micropollutants in 76 Wastewater Treatment Plants. *Process. Saf. Environ. Prot.* **2020**, *141*, 61–72. [CrossRef]
5. He, J.; Yang, X.; Men, B.; Wang, D. Interfacial mechanisms of heterogeneous Fenton reactions catalyzed by iron-based materials: A review. *J. Environ. Sci.* **2016**, *39*, 97–109. [CrossRef]
6. López-Vinent, N.; Cruz-Alcalde, A.; Gutiérrez, C.; Marco, P.; Giménez, J.; Esplugas, S. Micropollutant removal in real WW by photo-Fenton (circumneutral and acid pH) with BLB and LED lamps. *Chem. Eng. J.* **2020**, *379*, 122416. [CrossRef]
7. Díaz-Angulo, J.; Cotillas, S.; Gomes, A.I.; Miranda, S.M.; Mueses, M.; Machuca-Martínez, F.; Rodrigo, M.A.; Boaventura, R.A.; Vilar, V.J. A tube-in-tube membrane microreactor for tertiary treatment of urban wastewaters by photo-Fenton at neutral pH: A proof of concept. *Chemosphere* **2020**, *263*, 128049. [CrossRef] [PubMed]
8. Clarizia, L.; Russo, D.; Di Somma, I.; Marotta, R.; Andreozzi, R. Homogeneous photo-Fenton processes at near neutral pH: A review. *Appl. Catal. B Environ.* **2017**, *209*, 358–371. [CrossRef]
9. Arzate, S.; Campos-Mañas, M.; Miralles-Cuevas, S.; Agüera, A.; Sánchez, J.G.; Pérez, J.S. Removal of contaminants of emerging concern by continuous flow solar photo-Fenton process at neutral pH in open reactors. *J. Environ. Manag.* **2020**, *261*, 110265. [CrossRef]
10. Lin, H.H.-H.; Lin, A.Y.-C. Solar photo-Fenton oxidation of cytostatic drugs via Fe(III)-EDDS at circumneutral pH in an aqueous environment. *J. Water Process. Eng.* **2021**, *41*, 102066. [CrossRef]
11. Dong, W.Y. Jin, K. Zhou, S.P. Sun, Y. Li, X.D. Chen, Efficient degradation of pharmaceutical micropollutants in water and wastewater by FeIII-NTA-catalyzed neutral photo-Fenton process. *Sci. Total Environ.* **2019**, *688*, 513–520. [CrossRef] [PubMed]
12. Oller, I.; Malato, S. Photo-Fenton applied to the removal of pharmaceutical and other pollutants of emerging concern. *Curr. Opin. Green Sustain. Chem.* **2021**, *29*, 100458. [CrossRef]
13. García, L.; Leyva-Díaz, J.C.; Díaz, E.; Ordóñez, S. A review of the adsorption-biological hybrid processes for the abatement of emerging pollutants: Removal efficiencies, physicochemical analysis, and economic evaluation. *Sci. Total. Environ.* **2021**, *780*, 146554. [CrossRef]
14. Telgmann, U.; Borowska, E.; Felmeden, J.; Frechen, F.-B. The locally resolved filtration process for removal of phosphorus and micropollutants with GAC. *J. Water Process. Eng.* **2020**, *35*, 101236. [CrossRef]
15. Paredes, L.; Alfonsin, C.; Allegue, T.; Omil, F.; Carballa, M. Integrating granular activated carbon in the post-treatment of membrane and settler effluents to improve organic micropollutants removal. *Chem. Eng. J.* **2018**, *345*, 79–86. [CrossRef]
16. Mo, W.; Cornejo, P.K.; Malley, J.P.; Kane, T.E.; Collins, M.R. Life cycle environmental and economic implications of small drinking water system upgrades to reduce disinfection byproducts. *Water Res.* **2018**, *143*, 155–164. [CrossRef]
17. Durna, E.; Erkişi, E.; Genç, N. Regeneration of diclofenac-spent granular activated carbon by sulphate radical based methods: Multi-response optimisation of adsorptive capacity and operating cost. *Int. J. Environ. Anal. Chem.* **2020**, *102*, 4695–4709. [CrossRef]
18. Larasati, A.; Fowler, G.D.; Graham, N.J. Extending granular activated carbon (GAC) bed life: A column study of in-situ chemical regeneration of pesticide loaded activated carbon for water treatment. *Chemosphere* **2021**, *286*, 131888. [CrossRef]
19. Genç, N.; Durna, E.; Erkişi, E. Optimization of the adsorption of diclofenac by activated carbon and the acidic regeneration of spent activated carbon. *Water Sci. Technol.* **2020**, *83*, 396–408. [CrossRef]
20. Michael, S.G.; Michael-Kordatou, I.; Beretsou, V.G.; Jäger, T.; Michael, C.; Schwartz, T.; Fatta-Kassinos, D. Solar photo-Fenton oxidation followed by adsorption on activated carbon for the minimisation of antibiotic resistance determinants and toxicity present in urban wastewater. *Appl. Catal. B Environ.* **2019**, *244*, 871–880. [CrossRef]
21. Della-Flora, A.; Wilde, M.L.; Thue, P.S.; Lima, D.; Lima, E.C.; Sirtori, C. Combination of solar photo-Fenton and adsorption process for removal of the anticancer drug Flutamide and its transformation products from hospital wastewater. *J. Hazard. Mater.* **2020**, *396*, 122699. [CrossRef]
22. Khalil, A.; Nasser, W.S.; Osman, T.; Toprak, M.S.; Muhammed, M.; Uheida, A. Surface modified of polyacrylonitrile nanofibers by TiO2/MWCNT for photodegradation of organic dyes and pharmaceutical drugs under visible light irradiation. *Environ. Res.* **2019**, *179*, 108788. [CrossRef]
23. Gemeay, A.H.; El-Halwagy, M.E.; El-Sharkawy, R.G.; Zaki, A.B. Chelation mode impact of copper(II)-aminosilane complexes immobilized onto graphene oxide as an oxidative catalyst. *J. Environ. Chem. Eng.* **2017**, *5*, 2761–2772. [CrossRef]
24. Liao, H.; Stenman, D.; Jonsson, M. Study of Indigo carmine as radical probe in photocatalysis. *J. Photochem. Photobiol. A Chem.* **2009**, *202*, 86–91. [CrossRef]

25. Azam, K.; Shezad, N.; Shafiq, I.; Akhter, P.; Akhtar, F.; Jamil, F.; Shafique, S.; Park, Y.-K.; Hussain, M. A review on activated carbon modifications for the treatment of wastewater containing anionic dyes. *Chemosphere* **2022**, *306*, 135566. [CrossRef]
26. Chowdhury, M.F.; Khandaker, S.; Sarker, F.; Islam, A.; Rahman, M.T.; Awual, M.R. Current treatment technologies and mechanisms for removal of indigo carmine dyes from wastewater: A review. *J. Mol. Liq.* **2020**, *318*, 114061. [CrossRef]
27. El-Kammah, M.; Elkhatib, E.; Gouveia, S.; Cameselle, C.; Aboukila, E. Enhanced removal of Indigo Carmine dye from textile effluent using green cost-efficient nanomaterial: Adsorption, kinetics, thermodynamics and mechanisms. *Sustain. Chem. Pharm.* **2022**, *29*, 100753. [CrossRef]
28. Tien, H.N.; Bui, D.N.; Manh, T.D.; Tram, N.T.; Ngo, V.D.; Mwazighe, F.M.; Hoang, H.Y.; Le, V.T. Electrochemical degradation of indigo carmine, P-nitrosodimethylaniline and clothianidin on a fabricated Ti/SnO2–Sb/Co-βPbO2 electrode: Roles of radicals, water matrices effects and performance. *Chemosphere* **2023**, *313*, 137352. [CrossRef] [PubMed]
29. Lekshmi, K.V.; Yesodharan, S.; Yesodharan, E. MnO2 efficiently removes indigo carmine dyes from polluted water. *Heliyon* **2018**, *4*, e00897. [CrossRef] [PubMed]
30. Ghanmi, I.; Sassi, W.; Oulego, P.; Collado, S.; Ghorbal, A.; Díaz, M. Optimization and comparison study of adsorption and photosorption processes of mesoporous nano-TiO2 during discoloration of Indigo Carmine dye. *Microporous Mesoporous Mater.* **2022**, *342*, 112138. [CrossRef]
31. Saikam, L.; Arthi, P.; Jayram, N.D.; Sykam, N. Rapid removal of organic dyes from aqueous solutions using mesoporous exfoliated graphite. *Diam. Relat. Mater.* **2022**, *130*, 109480. [CrossRef]
32. De la Cruz, N.; Esquius, L.; Grandjean, D.; Magnet, A.; Tungler, A.; de Alencastro, L.; Pulgarín, C. Degradation of emergent contaminants by UV, UV/H2O2 and neutral photo-Fenton at pilot scale in a domestic wastewater treatment plant. *Water Res.* **2013**, *47*, 5836–5845. [CrossRef]
33. Miklos, D.B.; Hartl, R.; Michel, P.; Linden, K.G.; Drewes, J.E.; Hübner, U. UV/H2O2 process stability and pilot-scale validation for trace organic chemical removal from wastewater treatment plant effluents. *Water Res.* **2018**, *136*, 169–179. [CrossRef]
34. Zietzschmann, F.; Müller, J.; Sperlich, A.; Ruhl, A.S.; Meinel, F.; Altmann, J.; Jekel, M. Rapid small-scale column testing of granular activated carbon for organic micro-pollutant removal in treated domestic wastewater. *Water Sci. Technol.* **2014**, *70*, 1271–1278. [CrossRef]
35. Ramos, R.O.; Albuquerque, M.V.; Lopes, W.S.; Sousa, J.T.; Leite, V.D. Degradation of indigo carmine by photo-Fenton, Fenton, H2O2/UV-C and direct UV-C: Comparison of pathways, products and kinetics. *J. Water Process. Eng.* **2020**, *37*, 101535. [CrossRef]
36. Wroch, E. *Adsorption Technology in Water Treatment: Fundamentals, Processes and Modeling*, 2nd ed.; De Gruyter: Berlin, Germany, 2021.
37. Kumar, J.A.; Kumar, P.S.; Krithiga, T.; Prabu, D.; Amarnath, D.J.; Sathish, S.; Venkatesan, D.; Hosseini-Bandegharaei, A.; Prashant, P. Acenaphthene adsorption onto ultrasonic assisted fatty acid mediated porous activated carbon-characterization, isotherm and kinetic studies. *Chemosphere* **2021**, *284*, 131249. [CrossRef]
38. Katsigiannis, A.; Noutsopoulos, C.; Mantziaras, J.; Gioldasi, M. Removal of emerging pollutants through Granular Activated Carbon. *Chem. Eng. J.* **2015**, *280*, 49–57. [CrossRef]
39. Sun, Y.; Pignatello, J.J. Photochemical reactions involved in the total mineralization of 2,4-D by iron(3+)/hydrogen peroxide/UV. *Environ. Sci. Technol.* **1993**, *27*, 304–310. [CrossRef]
40. Arslan-Alaton, I.; Tureli, G.; Olmez-Hanci, T. Treatment of azo dye production wastewaters using Photo-Fenton-like advanced oxidation processes: Optimization by response surface methodology. *J. Photochem. Photobiol. A Chem.* **2009**, *202*, 142–153. [CrossRef]
41. Mitsika, E.E.; Christophoridis, C.; Kouinoglou, N.; Lazaridis, N.; Zacharis, C.K.; Fytianos, K. Optimized Photo-Fenton degradation of psychoactive pharmaceuticals alprazolam and diazepam using a chemometric approach—Structure and toxicity of transformation products. *J. Hazard. Mater.* **2020**, *403*, 123819. [CrossRef] [PubMed]
42. Palma-Goyes, R.E.; Silva-Agredo, J.; González, I.; Torres-Palma, R.A. Comparative degradation of indigo carmine by electrochemical oxidation and advanced oxidation processes. *Electrochimica Acta* **2014**, *140*, 427–433. [CrossRef]
43. Lumbaque, E.C.; Araújo, D.S.; Klein, T.M.; Tiburtius, E.R.L.; Argüello, J.; Sirtori, C. Solar photo-Fenton-like process at neutral pH: Fe(III)-EDDS complex formation and optimization of experimental conditions for degradation of pharmaceuticals. *Catal. Today* **2019**, *328*, 259–266. [CrossRef]
44. Land Brandenburg. Strategischen Gesamtplan zur Senkung der Bergbaubedingten Stoffeinträge in die Spree und deren Zuflüsse in der Lausitz. 2015. Available online: https://mluk.brandenburg.de/mluk/de/umwelt/wasser/bergbaufolgen-fuer-den-wasserhaushalt/# (accessed on 9 February 2024).
45. Nippes, R.P.; Macruz, P.D.; Scaliante, M.H.N.O. Toxicity reduction of persistent pollutants through the photo-fenton process and radiation/H2O2 using different sources of radiation and neutral pH. *J. Environ. Manag.* **2021**, *289*, 112500. [CrossRef] [PubMed]
46. Mejri, A.; Soriano-Molina, P.; Miralles-Cuevas, S.; Pérez, J.A.S. Fe3+-NTA as iron source for solar photo-Fenton at neutral pH in raceway pond reactors. *Sci. Total. Environ.* **2020**, *736*, 139617. [CrossRef] [PubMed]
47. Soriano-Molina, P.; De la Obra, I.; Miralles-Cuevas, S.; Gualda-Alonso, E.; López, J.C.; Pérez, J.S. Assessment of different iron sources for continuous flow solar photo-Fenton at neutral pH for sulfamethoxazole removal in actual MWWTP effluents. *J. Water Process. Eng.* **2021**, *42*, 102109. [CrossRef]
48. Nunes, K.G.P.; Sfreddo, L.W.; Rosset, M.; Féris, L.A. Efficiency evaluation of thermal, ultrasound and solvent techniques in activated carbon regeneration. *Environ. Technol.* **2020**, *42*, 4189–4200. [CrossRef]

49. Kempisty, D.M.; Arevalo, E.; Spinelli, A.M.; Edeback, V.; Dickenson, E.R.V.; Husted, C.; Higgins, C.P.; Summers, R.S.; Knappe, D.R.U. Granular activated carbon adsorption of perfluoroalkyl acids from ground and surface water. *AWWA Water Sci.* **2022**, *4*, e1269. [CrossRef]
50. Dutta, T.; Kim, T.; Vellingiri, K.; Tsang, D.C.; Shon, J.; Kim, K.-H.; Kumar, S. Recycling and regeneration of carbonaceous and porous materials through thermal or solvent treatment. *Chem. Eng. J.* **2019**, *364*, 514–529. [CrossRef]
51. Han, C.-H.; Park, H.-D.; Kim, S.-B.; Yargeau, V.; Choi, J.-W.; Lee, S.-H.; Park, J.-A. Oxidation of tetracycline and oxytetracycline for the photo-Fenton process: Their transformation products and toxicity assessment. *Water Res.* **2020**, *172*, 115514. [CrossRef]
52. Lumbaque, E.C.; Becker, R.W.; Araújo, D.S.; Dallegrave, A.; Ost Fracari, T.; Lavayen, V.; Sirtori, C. Degradation of pharmaceuticals in different water matrices by a solar homo/heterogeneous photo-Fenton process over modified alginate spheres. *Environ. Sci. Pollut. Res.* **2019**, *26*, 6532–6544. [CrossRef]
53. Belalcázar-Saldarriaga, A.; Prato-Garcia, D.; Vasquez-Medrano, R. Photo-Fenton processes in raceway reactors: Technical, economic, and environmental implications during treatment of colored wastewaters. *J. Clean. Prod.* **2018**, *182*, 818–829. [CrossRef]
54. Miralles-Cuevas, S.; Oller, I.; Agüera, A.; Pérez, J.A.S.; Sánchez-Moreno, R.; Malato, S. Is the combination of nanofiltration membranes and AOPs for removing microcontaminants cost effective in real municipal wastewater effluents? *Environ. Sci. Water Res. Technol.* **2016**, *2*, 511–520. [CrossRef]